DNA ORGANIZATION IN THE MATURE

SPERM OF SEVERAL ORTHOPTERA BY THE METHOD

OF POLARIZED FLUORESCENCE MICROSCOPY

JAMES W. MACINNES and ROBERT B. URETZ

From the Department of Biophysics, The University of Chicago, Chicago, Illinois 60637. Dr. MacInnes' present address is the Institute for Developmental Biology, University of Colorado, Boulder, Colorado 80302

ABSTRACT

Mature sperm of *Acheta domesticus, Acheta assimilis, Nemobius fasciatus, Nemobius confusus, Melanoplus femur-rubrum, Romalea microptera, Scudderia curvicauda*, and *Ceuthophilus nigricans* were examined for DNA configuration by means of polarized fluorescence microscopy. In all cases, the results suggest that the DNA lies in unsupercoiled array, predominantly parallel to the elongate sperm head axes. Detailed calculations of the factors influencing the degree of polarization of the fluorescent emission from supercoiled DNA are contained in an appendix.

INTRODUCTION

We have previously reported a technique for the determination of DNA organization in microscopic preparations, involving polarized fluorescence microscopy, which was utilized to determine DNA orientation in the salivary gland chromosomes of *Drosophila* (1). This technique utilizes the fact that the fluorescent dye acridine orange (AO) binds to native DNA in such a way that the flat planes of the dye molecules are rigidly held perpendicular to the DNA helix axis (for appropriately low dye-to-DNA concentrations). A large amount of evidence has been presented which supports an intercalation model for this binding mode (see, for example, 2 and 3 for references to this evidence). Fluorescence from an AO molecule occurs primarily with the E-vectors of the emitted light polarized parallel to the dye molecular plane. Therefore, fluorescence from AO, bound as above to a parallel array of native DNA helices, is plane-polarized with E-vectors predominantly perpendicular to the DNA helix axes.

The maximum amount of polarization to be expected is highly dependent upon the supercoiling of the DNA. This dependence is of especial interest in studies of sperm DNA packing, inasmuch as Inoué and Sato, utilizing patterns of loss of birefringence following polarized UV irradiation, have invoked a supercoiling model for the DNA packing in the head of the sperm of the cave cricket (*Ceuthophilus nigricans*) (4, 5). The relationship between supercoiling and the maximum degree of polarization, as well as the influence of several other factors, are discussed in detail in the Appendix.

Using the polarization of fluorescence technique, we have examined the sperm of *C. nigricans*, and of several other species of Orthoptera, for total DNA orientation. In addition, sperm heads of one species, *Acheta domesticus* (the house cricket), were scanned along their length with 0.5 μ resolution to look for localized changes in the DNA orientation.

MATERIALS AND METHODS

Instrumentation

The polarized fluorescence microscope used in this study has been described in detail elsewhere (3). Basically, it consists of a fluorescence microscope with a rotating (20 rpm) polaroid situated above the ocular, and a photomultiplier tube above the polaroid to measure light intensities. The signal is displayed as a chart recording. The microscope lenses employed were a 100X Zeiss oil immersion objective with an NA of 1.32, an inverted 43X American Optical objective of NA 0.66 serving as condenser, and an 8X Leitz ocular. The primary filter was a Corning 5-58, transmitting below 480 mμ, and the secondary filter was a Corning 3-69, transmitting above 510 mμ. Tilted glass plates serve to remove any polarization from the exciting light. An iris diaphragm located in an image plane above the ocular allows small areas of the field of view to be analyzed. Except for the scans of *A. domesticus*, discussed below, this aperture was set to include the whole or a large part of each head of each sperm. The apparatus used for spectral analysis was described previously (2).

For the scanning of the *A. domesticus* sperm heads, the diaphragm was replaced with a slit, situated so that its long axis was perpendicular to the long axis of the sperm head. The sperm head was scanned by employing a 1/90 rpm motor to drive a screw which advanced the microscope stage evenly, parallel to the long axis of the sperm head, at the rate of 5 μ/min. The slit width was set so that a 0.5 μ segment of the sperm head was seen.

Analysis of the Data

The degree of polarization of the fluorescence from a DNA-containing object, appropriately stained with AO, is analyzed by measuring the minimum and maximum intensities of emission as the polaroid is rotated, these intensities being measured from a background level determined by measuring the intensity of an "empty area" to one side of the object being analyzed.

R is defined as:

$$R = \frac{\text{maximum} - \text{minimum}}{\text{maximum}} \times 100\%,$$

with the following convention: if the maximum intensity is recorded when the transmitting axis of the polaroid is oriented perpendicular to the long axis of the object being measured, then R is positive. If the transmitting axis is parallel to the long axis of the object, then R is said to be negative. As will be seen, the sign of R is an important criterion in determining DNA supercoiling.
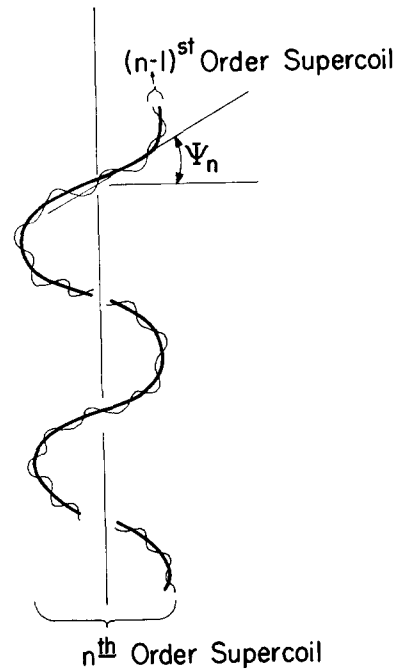

FIGURE 1   An nth-order supercoil, with a pitch angle ψ_n. It is constructed from an (n − 1)st-order supercoil. Native uncoiled DNA is considered an n = 0 supercoil. (Tan $\psi_n = P_n/2\,\pi r_n$, where P_n is the pitch, and r_n is the radius, of the nth-order coil.)

Detailed calculations of the effects upon R of the degree of supercoiling, of the pitch angle, ψ, associated with each order of coiling (see Fig. 1), and of the numerical aperture of the objective and of the condenser are given in the Appendix. The results of these calculations may be summarized as follows: the ideal maximum R values for the first three orders of supercoiling (straight native DNA is considered a zero-order coil) are $R_0 = 100\%$, $R_1 = -50\%$, $R_2 = 33\%$. The effect of the objective NA is to reduce these maximum values to $R_0 = 78.5\%$, $R_1 = -43.5\%$, $R_2 = 26.5\%$. Any effect of the condenser NA can only be to further decrease R. The effects of pitch angles are to reduce R's as the pitch angles increase. For example, for the pitch angles suggested by Inoué and Sato ($\psi_1 = 15°$, $\psi_2 = 10°$) for the second-order coiling of their model for *C. nigricans* sperm DNA, maximum R_2 is 19.2%. Therefore, any positive R found for *C. nigricans* sperm above 19.2% rules out Inoué and Sato's model for the pitch angles they suggest, and any R above 26.5% rules out a second-order supercoil altogether.

For an nth-order supercoil, the effect of the pitch angle, ψ_n, is to decrease the magnitude of R as ψ_n increases, until, at a certain value of ψ_n, R is reduced
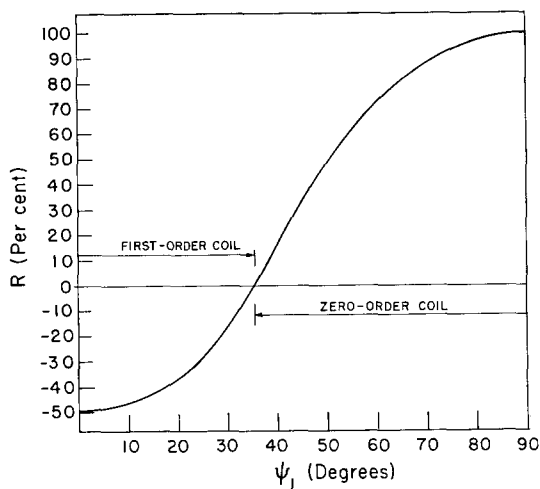
FIGURE 2 The effect of the pitch angle, ψ_1, upon R for a first-order supercoil. By the convention described in the text, the supercoil is considered a "wiggly" zero-order coil for ψ_1 above about 35°.

to zero. For larger ψ_n than this, R begins to increase in magnitude again, but with opposite sign. Therefore, the following convention is adopted: a supercoil is considered nth-order only as long as ψ_n is less than the pitch angle at which R is zero. For larger ψ_n, the supercoil is considered (n − 1) st-order with a "wiggle" in it given by ψ_n. Of course, in calculating the effect of ψ_n upon R, the equations for the nth-order coiling derived in the Appendix are used for all values of ψ_n from 0° to 90°. The effect of the first-order pitch angle upon R is illustrated for the ideal case (i.e. not considering numerical aperture effects) in Fig. 2. Beyond about 35°, R changes sign, so the coil is considered zero-order in that region.

Cytological Preparations

The mature sperm of *A. domesticus* and *A. assimilis* (the large black field cricket) were obtained from lightly anesthetized animals by dissecting out the spermatophores and placing them directly into 10^{-4} M AO (in 0.1 M acetate buffer, pH 4.5). The sperm-containing tubules ejaculated from the spermatophores directly into the AO solution, and were picked up with a pipette, placed on a slide, and lightly squashed in a drop of 1/10 SSC (saline sodium citrate). Sperm were obtained from anesthetized *Nemobius fasciatus* and *N. confusus* (field crickets), *Melanoplus femur-rubrum* (the common red-legged grasshopper), and *Scudderia curvicauda* (the bush katydid), by teasing apart the testes in the AO solution and mounting them as above.

Through the kindness of Drs. Inoué and Sato, a testis of *C. nigricans* was received preserved in 7.5%

dimethylsulfoxide. It was brought gradually to 1/10 SSC by ten successive two-fold dilutions, and then stained and mounted as above. The specimens of *Romalea microptera* (the southern lubber grasshopper) were purchased from General Biological Supply (Chicago, Ill.) and had been preserved by being dropped live into 95% ethanol. The testes were dissected out, and stained and mounted as above.

RESULTS

The R's obtained for the Orthoptera studied are given in Table I. It should be emphasized that these are over-all R's, that is, the R's associated with the entire sperm heads, and are, therefore, averages of all of the AO-bound DNA in each sperm head. In all cases, many sperm were analyzed; and with the exceptions of *R. microptera* and *C. nigricans*, sperm were taken from several animals. The values reported are the maximum R's obtained, but, in all cases, these differ from the mean values by less than 10%.

The results in Table I suggest that the DNA of all of the sperm examined, including those of *C. nigricans*, is packed in uncoiled (n = 0) array, primarily parallel to the elongate sperm head axes.

We made scans along the lengths of sperm heads of *A. domesticus*, to look for localized changes in R, perhaps corresponding to the packing of the ten chromosomes into the head in tandem, as was proposed for the grasshopper sperm by Taylor (6). One of these scans is shown in Fig. 3. No regular pattern of changes in R was noted from the scans.

DISCUSSION

These results are consistent with observations on the UV dichroism of grasshopper sperm by Caspersson (7), and on the X-ray diffraction patterns of squid sperm by Wilkins and Randall (8). They are in contradiction to the coiled-coil model of Inoué and Sato. However, it should be pointed out that Inoué and Sato arrived at their model in essentially two steps. The first step was the invocation of microdomains of zig-zag DNA to explain the pattern of loss of birefringence upon irradiation by polarized UV. The second step was the postulation of coiled-coiled DNA as a specific packing arrangement which would result in the zig-zag domains of the first step. Our results are not inconsistent with the existence of zig-zag microdomains; that is, our observed value of R for *C. nigricans* is sufficiently below the theoretical maximum for perfectly straight DNA to permit

Family	Genus	Species	Maximum R
			%
Gryllidae	Acheta	Domesticus	+56
Gryllidae	Acheta	Assimilis	+56
Gryllidae	Nemobius	Fasciatus	+46
Gryllidae	Nemobius	Confusus	+40
Acrididae	Melanoplus	Femur-rubrum	+64
Acrididae	Romalea	Microptera	+37
Tettigoniidae	Ceuthophilus	Nigricans	+67
Tettigoniidae	Scudderia	Curvicauda	+54

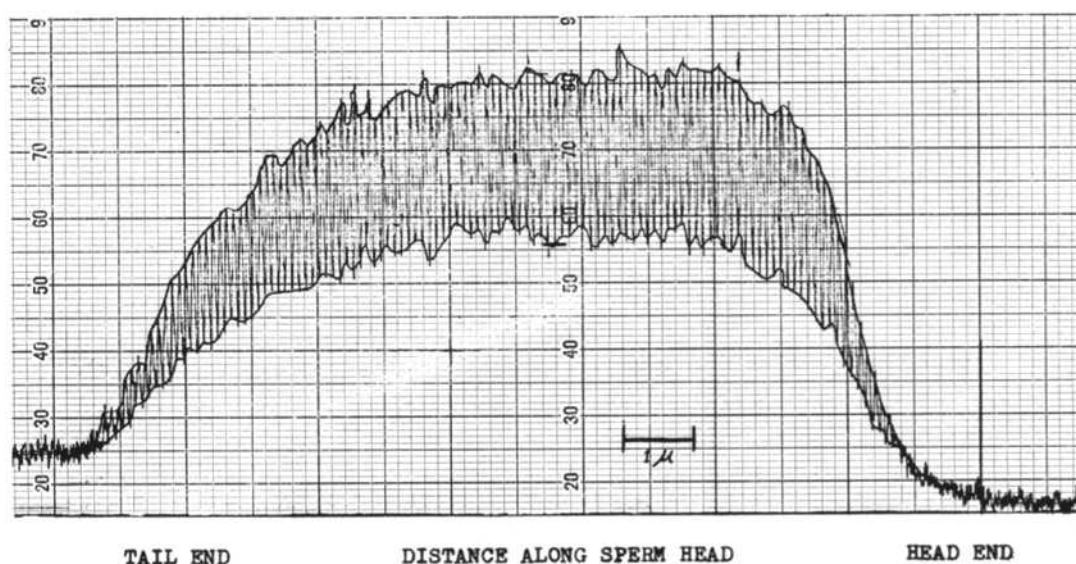TAIL END   DISTANCE ALONG SPERM HEAD   HEAD END

FIGURE 3 A scan along the length of an *A. domesticus* mature sperm head of the intensity of fluorescent emission as the polaroid above the eyepiece rotates. The large oscillations indicate the considerable polarization of the fluorescence. The envelope surrounding these oscillations was drawn in subsequently. The resolution of analysis is about 0.5 μ in the direction parallel to the elongate head axis. No significant alterations in R along the head are apparent. (As a result of the mechanical response time of the recorder used in these studies, the oscillations obtained on this chart recording are 16% less than the true amplitude of the oscillatory component of the signal produced. This factor was taken into account when determining minimum and maximum intensities from a chart recording.)

such zig-zags. Our results, however, are inconsistent with second-order supercoiling of the DNA as a way of arriving at the microdomains. It should also be emphasized that a requirement for the absence of coiling does not preclude extensive folding of the DNA back and forth in directions predominantly parallel to the sperm axis.

Of course, two basic assumptions are made if the polarized fluorescence microscopy technique is used for determination of DNA configuration: first, that the AO "samples" all orientations of the DNA in the object equally; second, that the AO binding does not seriously affect pre-existing DNA configuration. It has been shown that the binding of an intercalating molecule (ethidium bromide) to extracted intact polyoma DNA is both dependent upon and changes the degree of supercoiling of the DNA in solution (9); and that
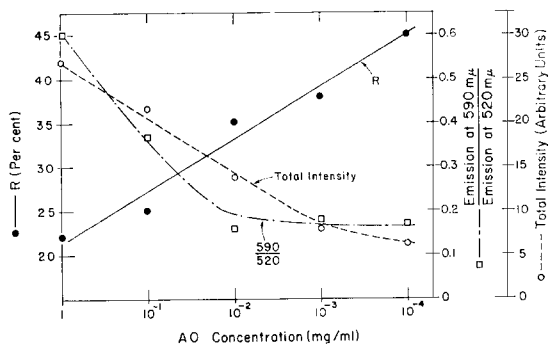
FIGURE 4 The relations between the AO concentration used to stain A. domesticus mature sperm and: the R value (the degree of fluorescence polarization), the total fluorescent intensity, and the ratio of emission at 590 mμ to that at 520 mμ. The 590/520 ratio is a measure of the ratio of "stacked" to monomeric dye molecules, which in turn is roughly a measure of the ratio of "side-bound" to intercalated dye. The sperm were stained for 30 sec in the AO solutions, which were made up to 0.1 M acetate buffer, pH 4.5.

the binding of AO to T4 DNA condensed in the phage head is markedly different from binding to free DNA (Dusenbery and Uretz, unpublished data).

With respect to the first assumption, it is difficult to imagine that the AO would not sample equally all positions in a given supercoil gyre, at least for the first order of coiling. Further, stained sperm do not have the appearance of "hollow tubes," as would be expected if the dye were sampling only the outside of the DNA package. Also, we have found that there is no difference in R between staining the sperm with low dye concentrations, or staining them with high AO concentrations followed by alcohol destaining.

With respect to the second assumption, it is strongly probable that the tight packing of DNA into the sperm head affects the amount of dye bound to the DNA. For example, Gledhill et al. (10) report a decrease in the binding of AO by DNA during the maturation of bull sperm. However, it is unlikely that the binding of the dye seriously affects the pre-existing configurations of highly condensed cytological DNA, especially in such fashion as to produce orientation of the DNA leading to a great increase in R. As can be seen in Fig. 4, R is highest at low dye concentrations.

We also require that there be no significant contribution to the polarized emission from AO

bound to substrates other than DNA, such as to give rise to higher R values than could be expected from dye bound to the DNA itself. Inspection of stained sperm subjected to various treatments and observations on isolated membranes, tubules, and tail fibers seem to bear out this assumption.

The lack of evidence for tandem packing of chromosomes in A. domesticus sperm by the scanning method is not sufficient to rule it out. It is possible that the resolution of 0.5 μ is not fine enough to detect the chromosome junctions, or perhaps there is considerable interpenetration of the chromosomes. A. domesticus, however, has a relatively wide and short sperm head compared to that of the grasshopper. It is possible that, while the chromosomes are in tandem in the grasshopper sperm, they are side by side in the house cricket sperm head.

APPENDIX

In this Appendix some of the effects of factors influencing R will be derived; the results will set upper limits on R's for zero-, first-, and second-order DNA supercoils analyzed by real optical systems. Similar calculations can be made for models of DNA configuration other than supercoiling; many such reduce to the same equations as found for supercoiling. For example, a "test-tube brush" radial array of DNA is equivalent to a first-order supercoil.

Our original estimate of R for an nth-order supercoil of DNA-AO was (1):

$$R_n = (-\tfrac{1}{2})^n \ 100\%,$$

based on the following highly simplified model. One starts with an (n − 1)st-order supercoil lying in a plane perpendicular to the viewing axis, with an R of R_{n-1}, and bends it into a circle in the plane parallel to the viewing axis. In a small segment at the top (or bottom) of this nth-order coil, one sees essentially straight (n − 1)st-order coils, running at right angles to the nth-order coil axis. At the outer edges of the nth-order coil, one is looking down at essentially cross-sections of the (n − 1)st-order coils, which are coming straight up (parallel to the viewing axis). It is clear that the cross-section of any coil gives an R of zero, while the segment at the top (or bottom) of the nth-order coil, being just a parallel array of (n − 1)st-order coils, gives an R of $-R_{n-1}$. Therefore, averaging the R's from

the segments all around the nth-order coil should give approximately:

$$R_n = -\tfrac{1}{2} R_{n-1},$$

the minus sign indicating that the direction of the maximum has changed. It is clear that a zero-order coil (straight double-stranded DNA) has an R of 100%, since all the dye molecules are standing on edge with their planes parallel, and the "minimum" intensity is zero.

This simplified model is, of course, not correct in the real case. As previously mentioned, among the factors influencing R are helix pitch angles for each coiling, differences in contributions to intensity from dye molecules in different orientations, the numerical aperture of the objective lens, the numerical aperture of the condenser, lack of infinite dichroic ratio, lack of perfect intercalation by the AO molecules, and "scatter" (due to reflections at lens surfaces, etc.). The last three factors, which serve to lower R, cannot be calculated *a priori*, but all of the others will be, with the exception of the effect of the condenser, which will be estimated.

To begin a consideration of helix coilings in the real case, it is useful to replace considerations of the whole coil with equivalent operations on a single light emitter (a dye molecule) placed at the center of the coordinate system, and then to integrate the contributions from all such emitters in the population around one loop of the coil.

Consider first a vector, which represents an emitting dipole, with perpendicular components A_x, A_y, and A_z, and which will be assumed to have unit length (Fig. 5). It is assumed that this
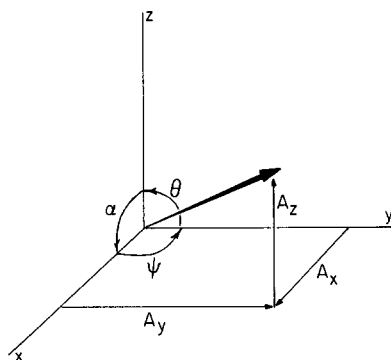

FIGURE 5 A vector of unit length in three-space, having components A_x, A_y, A_z, and showing the three rotations, α, ψ, θ.

vector is viewed from above, i.e. along the z-axis. It can be seen that an operation equivalent to coiling is performed on this vector by: (a) rotating the system about either the x-axis (θ rotation) or the y-axis (α rotation) to obtain new components $A_x{}'$, $A_y{}'$, and $A_z{}'$ for the vector; (b) integrating the square of each component (since the intensity is the square of the amplitude) over either θ or α from 0 to 2π, to obtain $I_x{}'$, $I_y{}'$, and $I_z{}'$, the light intensities for the whole loop of the coil. To introduce a pitch angle, one must (a) first rotate the vector about the z-axis by a fixed angle ψ, which is equal to the pitch angle, obtaining new components $\bar{A}_x$, $\bar{A}_y$, $\bar{A}_z$, for the vector; (b) perform the θ or α rotation above, to obtain components $\bar{A}'_x$, $\bar{A}'_y$, $\bar{A}'_z$; (c) integrate the square of each component over θ or α from 0 to 2π, to obtain intensities $\bar{I}'_x$, $\bar{I}'_y$, $\bar{I}'_z$.

Performing the rotations yields, for the θ rotation:

$$\bar{A}_x{}' = A_x \cos\psi - A_y \sin\psi$$

$$\bar{A}_y{}' = A_x \sin\psi \cos\theta + A_y \cos\psi \cos\theta$$

$$- A_z \sin\theta \qquad (1)$$

$$\bar{A}_z{}' = A_x \sin\psi \sin\theta + A_y \cos\psi \sin\theta$$

$$+ A_z \cos\theta,$$

while for the α rotation:

$$\bar{A}_x{}' = A_x \cos\psi \cos\alpha - A_y \sin\psi \cos\alpha$$

$$+ A_z \sin\alpha$$

$$\bar{A}_y{}' = A_x \sin\psi + A_y \cos\psi \qquad (2)$$

$$\bar{A}_z{}' = -A_x \cos\psi \sin\alpha + A_y \sin\psi \sin\alpha$$

$$+ A_z \cos\alpha.$$

It is of no value to perform the squarings and integrations at this point, since in the real cases various cross-terms will conveniently drop out upon integrating them over 2π.

Consider next the effect of the numerical aperture of the objective lens. It is clear that this effect is due to the fact that the lens "views" the light vectors from directions off of the z-axis. Therefore, for instance, from a direction off of the z-axis but directly above the x-axis, the lens sees a portion of the z-component and adds it to the x-component, while seeing the x-component less.

For calculation of the effect of numerical aperture on the various components, producing new components $\bar{A}_x''$ and $\bar{A}_y''$ in the image plane where polarization analysis takes place, it is useful to consider separately how each of $\bar{A}_x'$, $\bar{A}_y'$, and $\bar{A}_z'$ contributes to the new components. For a viewing direction off of the z-axis and defined by the angles β, γ, the contributions to $\bar{A}_x''$ and $\bar{A}_y''$ from $\bar{A}_x'$ and from $\bar{A}_y'$ are analyzed in Figs. 6 and 7 (the contributions from $\bar{A}_x'$ are obviously obtained like those from $\bar{A}_y'$). Altogether:

$$\bar{A}_x'' = \bar{A}_x' \,(\sin^2 \beta + \cos^2 \beta \cos \gamma)$$
$$+ \bar{A}_y' \,(\sin \beta \cos \beta \cos \gamma - \sin \beta \cos \beta)$$
$$- \bar{A}_z' \,(\cos \beta \sin \gamma)$$

$$\bar{A}_y'' = \bar{A}_x' \,(\sin \beta \cos \beta \cos \gamma - \sin \beta \cos \beta)$$
$$+ \bar{A}_y' \,(\sin^2 \beta \cos \gamma + \cos^2 \beta)$$
$$- \bar{A}_z' \,(\sin \beta \sin \gamma).$$

In this last derivation, we have ignored the differences in transmission that occur in the outer quadrants of the lens aperture for light polarized in different directions. Although these differences are an important source of depolarization in transmission polarization microscopy, they make a negligible contribution to the large amount of depolarization to be found for self-luminous objects.
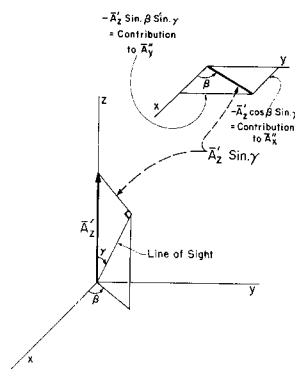
It is of value to perform at this point the integra-

FIGURE 6   The contributions of $\bar{A}_z'$ to $\bar{A}_x''$ and $\bar{A}_y''$ when viewed from a direction, β, γ. The vector $\bar{A}_z'$ is broken down into two perpendicular vectors, one of which is parallel to the line of sight, and is, therefore, not "seen" by the lens. The other vector is bent up by the lens into the x-y plane at the image plane, and is there divided into x and y components (upper right inset).
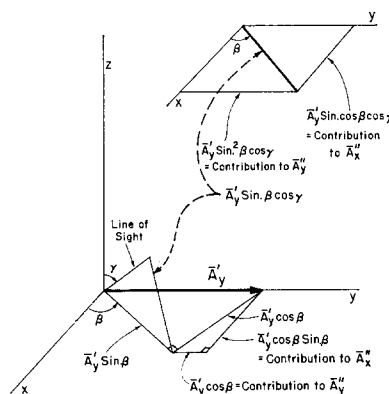

FIGURE 7   The contributions of $\bar{A}_y'$ to $\bar{A}_x''$ and $\bar{A}_y''$ when viewed from a direction β, γ. The vector $\bar{A}_y'$ is broken down into three mutually perpendicular vectors, one of which is parallel to the line of sight, and, therefore, not seen by the lens. Another lies in the x-y plane and is transmitted unchanged by the lens, and so may be broken down into x and y components as is. The third is bent up by the lens into the x-y plane at the image plane, and is there divided into x and y components (inset at upper right).

tions over β and γ. The cone of light from the specimen which the objective lens sees is limited by the numerical aperture of the lens and by the indices of refraction of intervening materials. This cone is defined by its half-angle, Φ. Φ is the maximum value of γ in Figs. 6 and 7. Therefore, the integration over γ is from 0 to Φ, and for β, from 0 to 2π; the integration is over the area of an imaginary inverted bowl with the z-axis passing through its center, representing the portion of the sphere of emitted light which is seen by the objective. An area element of this bowl (of unit radius) is $\sin \gamma \, d\beta d\gamma$, so:

$$\bar{I}_x'' = (2\pi)^{-1} \iint (\bar{A}_x'')^2 \sin \gamma d\beta d\gamma$$

$$\bar{I}_y'' = (2\pi)^{-1} \iint (\bar{A}_y'')^2 \sin \gamma d\beta d\gamma.$$

The $(2\pi)^{-1}$ is used to avoid carrying constant "π" terms along; this will have no effect on R, since it will cancel out when that calculation is made. These integrations may be performed, and the effect of Φ on $(\bar{I}_x'' - \bar{I}_y'')/\bar{I}_x''$ for this arbitrary emitting dipole calculated. While $\bar{I}_x''$ may not be in the direction of the maximum intensity for an arbitrary dipole, $\bar{I}_x''$, or $\bar{I}_y''$ if ψ is large, for the whole assemblage of dipoles will

be, as a result of the direction chosen for the zero-order DNA helix axis, as will be seen later. Therefore, for ψ not so large that $\bar{I}_y{}'' > \bar{I}_{x'}{}''$:

$$R = (\bar{I}_x{}'' - \bar{I}_y{}'') \div (\bar{I}_x{}'')$$

$$= (\bar{I}_x{}' - \bar{I}_y{}')(\tfrac{7}{12} - \tfrac{1}{4}\cos\Phi - \tfrac{1}{4}\cos^2\Phi$$

$$- \tfrac{1}{12}\cos^3\Phi) \div [\bar{I}_x{}'(\tfrac{5}{8} - \tfrac{3}{8}\cos\Phi$$

$$- \tfrac{1}{8}\cos^2\Phi - \tfrac{1}{8}\cos^3\Phi) + \bar{I}_y{}'(\tfrac{11}{24}$$ (3)

$$- \tfrac{1}{8}\cos\Phi + \tfrac{1}{8}\cos^2\Phi - \tfrac{1}{24}\cos^3\Phi)$$

$$+ \bar{I}_z{}'(\tfrac{1}{3} - \tfrac{1}{2}\cos\Phi + \tfrac{1}{6}\cos^3\Phi)].$$

As a minor check on this, note that by cancelling $(1 - \cos\Phi)$, for $\Phi = 0$, $R = (\bar{I}_x{}' - \bar{I}_y{}')/(\bar{I}_x{}')$ as it should.

With the objective lens of the instrument used in these studies, Φ is $61°$. With this lens, therefore

$$R = 0.398\ (\bar{I}_x{}' - \bar{I}_y{}')$$

$$\div\ (0.407\bar{I}_x{}' + 0.009\bar{I}_y{}' + 0.100\bar{I}_z{}')$$ (4)

Returning now to the problem of supercoiling, one must work up from the n = 0 case, using Equations (1) and (2) to get from one coiling to the next higher one. It is assumed that the dye molecules sample all orientations of the DNA impartially and that the AO binding does not change the pre-existing DNA supercoiling. Also, because of the helical nature of native DNA, all positions of a dye molecule obtained by rotation about the axis perpendicular to its plane are equally probable. Therefore, the properties of the individual dipole moments to be associated with a single elliptical dye molecule each show circular symmetry when averaged over all of the dye molecules lying parallel to that plane.

We assume an infinite dichroic ratio, so that the emitting dipole always lies in the plane of the dye molecule. Also, for the sections immediately following, we assume that the probability of excitation of a particular dye molecule is independent of its orientation. This last assumption will be modified when we consider the effects of condenser aperture.

To begin, for the n = 0 case, the dye molecules are all oriented with their planes perpendicular to the $x - y$ plane (i.e. "on edge"), and parallel to the $x - z$ plane; that is, the DNA helix axis is parallel to the y-axis (see Fig. 8). It will become apparent (and can be shown rigorously) that, for
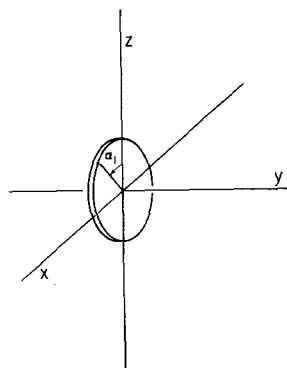

FIGURE 8 A disk, representing an AO molecule intercalated into a DNA helix, which has its axis along the y-axis. The AO molecules, therefore, all lie with their planes parallel to the x-z plane. Light may be emitted from any dipole lying in the molecular plane, and, therefore, the dipole can have any orientation, α_1. Of course, real dye molecules are elliptical rather than circular, but the averaging of all such molecules parallel to the x-z plane makes the dipole properties behave as though the molecules are all circular.

small ψ, the maximum intensity will always be parallel to the x-axis for all values of n. However, the direction of the coil axis shifts with each new supercoiling. Thus, for n = 0 and all other even values of n, the coil axis is parallel to the y-axis, while for n odd it is parallel to the x-axis. Therefore, R is positive (by the conventions described in the text) for even n, and negative for odd n. For large ψ, R will change sign, but, as discussed previously in the text, at this point an nth order supercoil is considered a wiggly (n − 1)st order supercoil, still describable by the equations for an nth order supercoil but with x and y axis interchanged in order to preserve the definition of R as (max-min)/max.

For the n = 0 case, there is no ψ_0, since it is assumed that the dye molecules are rigidly held by the DNA perpendicular to the DNA helix axis. For slight coiling, R_0 is affected as described by the equations below for the n = 1 case. For perfectly straight DNA ($\psi_1 = 90°$), a light-emitting dipole of unit length in the plane of the molecule, therefore, has an x-component of $\sin\alpha_1$ and a z-component of $\cos\alpha_1$; the y-component is zero (Fig. 8). Hence, since all values of α_1 are equally represented for the set of dipoles associated with dye molecules bound to a DNA helix, integrating α_1 from 0 to 2π:

$$\bar{I}_x' = (2\pi)^{-1} \int \sin^2 \alpha_1 \, d\alpha_1 = \frac{1}{2}$$

$$\bar{I}_y' = 0$$

$$\bar{I}_z' = (2\pi)^{-1} \int \cos^2 \alpha_1 \, d\alpha_1 = \frac{1}{2}.$$

These values can be substituted into Equations (3) and (4) to give:

$$R_0 = (\frac{7}{12} - \frac{1}{4} \cos \Phi - \frac{1}{4} \cos^2 \Phi - \frac{1}{12} \cos^3 \Phi)$$

$$\div (\frac{23}{24} - \frac{7}{8} \cos \Phi - \frac{1}{8} \cos^2 \Phi \qquad (5)$$

$$+ \frac{1}{24} \cos^3 \Phi)$$

for an arbitrary objective lens, and

$$R_0 = 78.5\% \qquad (6)$$

for the particular lens. For the idealized case of a lens with NA $\rightarrow$ 0, maximum R_0, (cancelling $[1 - \cos \phi]$), would, of course, be 100%.

Proceeding to the case of n = 1: this involves a θ rotation of the dye molecules, and, consequently, of the array of dipoles by which the molecules are represented, and introduces a pitch angle, ψ_1. Using Equation (1), therefore,

$$\bar{A}_x' = \sin \alpha_1 \cos \psi_1$$

$$\bar{A}_y' = \sin \alpha_1 \cos \theta_1 \sin \psi_1 - \cos \alpha_1 \sin \theta_1 \qquad (7)$$

$$\bar{A}_z' = \cos \alpha_1 \cos \theta_1 + \sin \alpha_1 \sin \theta_1 \sin \psi_1.$$

Integrate the square of these components over α_1 and θ_1, from 0 to 2π in both cases,

$$\bar{I}_x' = \frac{1}{2} \cos^2 \psi_1$$

$$\bar{I}_y' = \frac{1}{4} \sin^2 \psi_1 + \frac{1}{4}$$

$$\bar{I}_z' = \frac{1}{4} \sin^2 \psi_1 + \frac{1}{4}$$

These can be put into Equations (3) and (4) to obtain R_1 for arbitrary lens NA, and for the lens used. For an n = 1 coil with no pitch angle (ψ_1 = 0), maximum R_1 is -43.5% for the lens used; and for the idealized case of NA = 0, in addition to ψ_1 = 0, R_1 = -50%. It can be seen that a pitch angle will reduce the magnitude of R_1, as shown in Fig. 2.

The case of n = 2 is the last case of any immediate practical interest (because of Inoué and Sato's proposal of second-order supercoiling of

sperm DNA). For n = 2, $\bar{A}_x'$, $\bar{A}_y'$, and $\bar{A}_z'$ are obtained by substituting the components of Equation (7) into Equation (2) for a second α rotation, and including a second pitch angle, ψ_2. These are then squared and integrated over α_1, θ_1, and α_2, each from 0 to 2π, to give:

$$\bar{I}_x' = \frac{1}{8} + \frac{1}{4} \cos^2 \psi_1 \cos^2 \psi_2 + \frac{1}{8} \sin^2 \psi_1 \sin^2 \psi_2$$

$$+ \frac{1}{8} \sin^2 \psi_1 + \frac{1}{8} \sin^2 \psi_2$$

$$\bar{I}_y' = \frac{1}{4} \sin^2 \psi_1 \cos^2 \psi_2 + \frac{1}{2} \cos^2 \psi_1 \sin^2 \psi_2 \qquad (8)$$

$$+ \frac{1}{4} \cos^2 \psi_1$$

$$\bar{I}_z' = \bar{I}_x'.$$

These can now be substituted into Equations (3) and (4) to give R_2 for an arbitrary lens, and for the one used, respectively. For the case of this lens, for the n = 2 case with both pitch angles, ψ_1 and ψ_2, zero, maximum R_2 is 26.5%. For the idealized n = 2 case where ψ_1, ψ_2, and Φ are all zero, maximum R_2 is 33%. As was the case for n = 1, pitch angles reduce the value of R_2.

Consider briefly the problem of the numerical aperture of the condenser. So far it has been assumed that each dye molecule receives the same intensity of exciting light. The effect of a condenser which gives less than hemispherical illumination must be to reduce the R's for coiled DNA, since in this real case more light will be absorbed by molecules lying flat (i.e. parallel to the $x = y$ plane) than those on edge. Since the on-edge molecules contribute to R, while the flat ones reduce it, R must be reduced. This can be demonstrated as follows: for a light-absorbing dipole at the origin, the total absorption from a lens with an angle of illumination, Φ_c, is found by integrating the square of the dipole length, as seen from an arbitrary direction, β, γ, over an imaginary shell representing the emitting surface. β goes from 0 to 2π, γ from 0 to Φ_c. For the vertical and horizontal dipoles, the lengths as seen from β, γ for illumination with unpolarized light can be determined from Figs. 6 and 7, respectively. The square of the length of the vertical dipole seen from any β value is $\sin^2 \gamma$, while that of a horizontal dipole lying along the y-axis is ($\sin^2 \beta \cos^2 \gamma + \cos^2 \beta$). An area element on the surface of the imaginary emitting shell is $\sin \gamma \, d\beta d\gamma$. Therefore, the integrations for i_v and i_h (the absorptions for vertical and horizontal dipoles) are:

$$i_v = (2\pi)^{-1} \iint \sin^3 \gamma\, d\beta d\gamma$$

$$= 1/3 \left[2 - \cos \Phi_c \left(2 + \sin^2 \Phi_c\right)\right]$$

$$i_h = (2\pi)^{-1} \iint \left(\sin^2 \beta \sin \gamma \cos^2 \gamma\right.$$

$$\left. + \cos^2 \beta \sin \gamma\right) d\beta d\gamma$$

$$= 1/3 \left[2 - \cos \Phi_c \left(2 - \tfrac{1}{2} \sin^2 \Phi_c\right)\right].$$

It will be noted that the ratio, i_v/i_h, is 1.0 for $\Phi_c = 90°$ (hemispherical illumination) and is zero (using l'Hospital's rule) for $\Phi_c \rightarrow 0$ (i.e. the vertical dipole gets no radiation), as expected. If a dye molecule is pictured as having two perpendicular dipoles lying in its molecular plane, so that a flat molecule has two horizontal dipoles while an on-edge molecule has one horizontal and one vertical dipole, then the flat molecule receives $\tfrac{2}{3}[2 - \cos \Phi_c(2 - \tfrac{1}{2} \sin^2 \Phi_c)]$ amount of energy, while the on-edge molecule gets $\tfrac{2}{3}[2 - \cos \Phi_c(2 + \tfrac{1}{4} \sin^2 \Phi_c)]$. The condenser usually used in this work has an NA of 0.66. Hence, neglecting that the mounting medium may be of slightly different refractive index than the glass of the slides, $\Phi_c = 41.3°$. With this value, the ratio of the energy received by the on-edge molecule to that received by the flat one is 0.62. It is not clear that to attempt to apply this effect rigorously to the R equations derived above is worthwhile, since there may be energy transfer between molecules in different orientations, which would serve to reduce or eliminate the effect. However, a simple model will illustrate the approximate possible magnitude of the effect.

Taking a first-order supercoil, assume for simplicity that the population consists of one-half the dye molecules lying flat and one-half lying on edge, parallel to the x-axis. Thus, if all effects of pitch angle, objective aperture, and condenser

aperture are neglected, the R of this population is

$$R = -\frac{(\tfrac{1}{2} + \tfrac{1}{2}) - \tfrac{1}{2}}{(\tfrac{1}{2} + \tfrac{1}{2})} = -50\%,$$

since both the flat and the on-edge molecules contribute to I_x, while only the flat ones, i.e. half the total population, contribute to I_y. This value is the expected one for the idealized n = 1 case. The effect of the numerical aperture of the condenser used, then, is to affect R as follows:

$$R = \frac{0.62(\tfrac{1}{2}) + \tfrac{1}{2} - \tfrac{1}{2}}{0.62(\tfrac{1}{2}) + \tfrac{1}{2}} = -38.3\%,$$

a considerable effect. For a zero-order coil, the condenser aperture will have no effect, since all the molecules are equivalent and obtain the same amount of light. With a simplified model for the n = 2 case similar to the one above, R is reduced from an idealized value of 33 to 28%, for the condenser used.

It should be pointed out that, inasmuch as DNA base pairs are planar molecules oriented in the same directions as bound acridine orange, most of the equations derived in this appendix are also applicable to considerations of the maximum UV dichroism to be expected for different DNA configurations. The related question of the effect of coiling on the birefringence of DNA has been considered by Maestre and Kilkson (11).

REFERENCES

1. MacInnes, J. W., and R. B. Uretz. 1966. Organization of DNA in dipteran polytene chromosomes as indicated by polarized fluorescence microscopy. Science. 151:689.
2. MacInnes, J. W., and R. B. Uretz. 1966. Spectral analysis of the binding of acridine orange to polytene chromosomes. Proc. Natl. Acad. Sci. U.S. 55:1109.
3. MacInnes, J. W., and R. B. Uretz. 1967. Thermal depolarization of fluorescence from polytene chromosomes stained with acridine orange. J. Cell. Biol. 33:597.
4. Inoué, S., and H. Sato. 1962. Arrangement of DNA in living sperm: a biophysical analysis. Science. 136:1122.
5. Inoué, S., and H. Sato. 1966. Deoxyribonucleic

acid arrangement in living sperm. *In* Molecular Architecture in Cell Physiology. Hayashi and Szent-Györgyi, editors. Prentice-Hall, Inc., Englewood Cliffs, N. J. 209.

6. TAYLOR, J. H. 1964. The arrangement of chromosomes in the mature sperm of the grasshopper. *J. Cell Biol.* **21**:286.

7. CASPERSSON, T. 1940. Nukleinsäurekketten und genvermehrung. *Chromosomo.* **1**:605.

8. WILKINS, M. H. F., and J. T. RANDALL. 1953. Crystallinity in sperm heads, molecular structure of nucleoprotein *in vivo. Biochim. Biophys. Acta.* **10**:192.

9. CRAWFORD, L. V., and M. J. WARING. 1967. Supercoiling of polyoma virus DNA measured by its interaction with ethidum bromide. *J. Mol. Biol.* **25**:23.

10. GLEDHILL, B. L., M. P. GLEDHILL, R. RIGLER, JR., and N. R. RINGERTZ. 1966. Changes in deoxynucleoprotein during spermiogenesis in the bull. *Exptl. Cell Res.* **41**:652.

11. MAESTRE, M. F., and R. KILKSON. 1965. Intrinsic birefringence of multiple-coiled DNA, theory and applications. *Biophys. J.* **5**:275.